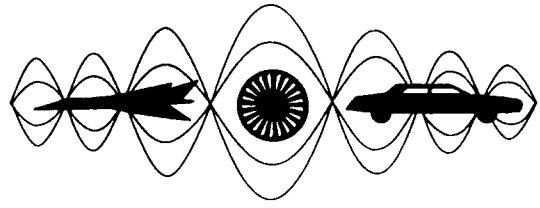

FIFTH INTERNATIONAL CONGRESS ON SOUND AND VIBRATION
DECEMBER 15-18, 1997
ADELAIDE, SOUTH AUSTRALIA

A WAVE BASED PREDICTION TECHNIQUE FOR VIBRO-ACOUSTIC SYSTEMS WITH CYLINDRICAL SHELL COMPONENTS

W. Desmet, P. Sas, D. Vandepitte

Department of Mechanical Engineering, Division PMA
Katholieke Universiteit Leuven, Belgium

Abstract

In a coupled vibro-acoustic analysis, the structural finite element model and acoustic finite or boundary element model must be solved simultaneously. This results in a very large, non-symmetrical coupled model, which requires a computationally expensive solving procedure. To reduce the size of a coupled model, a wave based modelling technique has been developed. Instead of dividing the structural and acoustic domain into small elements and solving the dynamic equations within each element using simple approximating shape functions, the entire structural and acoustic domain are described by wave functions, which are exact solutions of the structural and acoustic homogeneous wave equation. To these wave functions, particular solutions of the inhomogeneous wave equations are added, so that the governing dynamic equations are exactly satisfied. The contributions of the wave functions to the coupled vibro-acoustic response are determined by applying the boundary conditions in a weighted residual formulation. In this paper, the method is applied to the two-dimensional cases of an acoustic cavity, of which the whole boundary surface consists of a force excited cylindrical shell structure, as well as a cavity, of which only a part of the boundary surface consists of a force excited cylindrical shell section.

1. Introduction

When all structural and acoustic subsystems are finite in extent, the most appropriate prediction method for steady-state analysis is a finite element discretization of the structural and acoustic subsystems. In the finite element method, the continuous domain in which the dynamic variables are governed by the dynamic equations and boundary conditions, is discretized into a number of finite elements (mesh). Within each element, the dynamic variables are expressed as a combination of the prescribed shape functions of each node of the considered element, weighted by the corresponding nodal values. As the nodal shape

functions are not exact solutions of the dynamic wave equations, the finite element results yield only an approximation of the desired solution. As the shape functions are usually simple low order polynomial functions, the continuous domain must be split into a large number of elements to get an accurate representation of the spatial variation of the dynamic response. This results in a large model size, which requires a large amount of computational resources for building and solving the model. Since the structural and acoustic wavelengths decrease with frequency, the spatial variation of the dynamic response increases so that the mesh density and subsequent computational effort required for a given accuracy increases with frequency. Due to this increased computational effort, the application region of the finite element method is practically limited up to a certain frequency threshold. For coupled vibro-acoustic problems, this threshold is substantially lower compared to uncoupled structural or acoustic problems. On one hand, the coupled model size is substantially larger as the structural and acoustic problem must be solved simultaneously. On the other hand, the most commonly used coupled formulation - an Eulerian formulation[1], in which the fluid is described by the pressure while the structural components are described by a displacement vector - results in a non-symmetrical model, which requires a substantially larger computational effort, compared to a symmetrical uncoupled structural or acoustic model.
The aim of the wave based prediction technique is to obtain the same accuracy as the finite element method with a substantially smaller coupled vibro-acoustic model so that the practical frequency threshold of the method can be raised significantly. The principle of the wave method is to express the dynamic variables as a combination of plane structural and acoustic waves, which exactly satisfy the homogeneous wave equations. To these wave functions, particular solutions of the inhomogeneous wave equations are added, so that the governing dynamic equations are exactly satisfied. The contributions of the wave functions to the coupled vibro-acoustic response are determined by applying the boundary conditions in a weighted residual formulation. In this way, there will be only an approximation error on the vibro-acoustic response, if the boundary conditions are not exactly satisfied. As a result, a substantially smaller number of wave functions is required for a certain accuracy, compared to the number of finite element shape functions, which are no exact solutions.
A detailed discussion of the wave based prediction method is given elsewhere[2,3,4]. In this paper, the method is applied to vibro-acoustic systems with cylindrical shell components and a comparison with the finite element method is given for two numerical examples.

2. Wave model

2.1. Dynamic equations of a thin cylindrical shell

Consider an infinitesimal section of a thin cylindrical shell with radius a and thickness h, as shown on Fig. 1. It is assumed that there is no axial displacement, so that the shell displacements may be expressed in a two-dimensional co-ordinate system (φ,z) fixed at the shell middle surface. The radial and circumferential displacements of the shell middle surface are denoted by w and v, respectively. According to Love's cylindrical shell theory[5], the in plane circumferential strains ε_φ and normal stresses σ_φ are defined as

$$\varepsilon_\varphi = \frac{1}{a}\left(\frac{dv}{d\varphi} + w\right) - \frac{z}{a^2}\left(\frac{d^2w}{d\varphi^2} - \frac{dv}{d\varphi}\right) \quad \text{and} \quad \sigma_\varphi = \frac{E}{1-\nu^2}\varepsilon_\varphi, \tag{1,2}$$

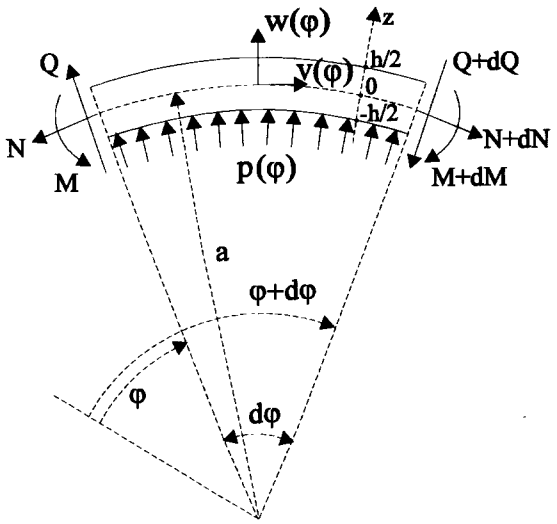

Fig. 1: infinitesimal cylindrical shell section

where E is the modulus of elasticity and ν is the Poisson coefficient of the shell material. By using Eqs. (1) and (2), the resulting normal force N and bending moment M, acting on the shell cross section, become

$$N = \int_{-h/2}^{h/2} \sigma_\varphi . dz = \frac{Eh}{(1-\nu^2)a}\left(\frac{dv}{d\varphi} + w\right), \qquad (3)$$

$$M = \int_{-h/2}^{h/2} \sigma_\varphi . z dz = -\frac{Eh^3}{12(1-\nu^2)a^2}\left(\frac{d^2w}{d\varphi^2} - \frac{dv}{d\varphi}\right). \qquad (4)$$

The resulting shear force Q is obtained from the momentum equilibrium, in which the rotational inertia is neglected,

$$Q = -\frac{1}{a}\frac{dM}{d\varphi}. \qquad (5)$$

The displacement components v and w due to an internal pressure excitation p are obtained from the dynamic force equilibrium in both the circumferential and radial direction. The resulting dynamic equations are

$$\rho h a \ddot{v} = \frac{dN}{d\varphi} + \frac{1}{a}\frac{dM}{d\varphi} \quad \text{and} \quad \rho h a \ddot{w} = pa + \frac{1}{a}\frac{d^2M}{d\varphi^2} - N, \qquad (6,7)$$

where ρ is the shell density and ¨ denotes the second time derivative.

To get the steady-state dynamic response, a harmonic time variation $e^{j\omega t}$ at frequency ω is assumed. Addition of the first derivative of Eq. (6) to Eq. (7) with the use of expressions (3) and (4) yields ($c_p^2 = \frac{E}{\rho(1-\nu^2)}$)

$$\left(1 - \frac{a^2\omega^2}{c_p^2}\right)N = pa + \frac{2}{a}\frac{d^2M}{d\varphi^2} + \frac{d^2N}{d\varphi^2}. \qquad (8)$$

Subtraction of the first derivative of Eq. (6) from the second derivative of Eq. (7) yields

$$\frac{d^2N}{d\varphi^2} = \frac{a}{2}\frac{d^2p}{d\varphi^2} - \frac{6a^3\omega^2}{c_p^2h^2}M - \frac{1}{2a}\frac{d^2M}{d\varphi^2} + \frac{1}{2a}\frac{d^4M}{d\varphi^4}. \qquad (9)$$

Substitution of Eq. (9) in Eq. (8) yields

$$\left(1 - \frac{a^2\omega^2}{c_p^2}\right)N = pa + \frac{a}{2}\frac{d^2p}{d\varphi^2} - \frac{6a^3\omega^2}{c_p^2h^2}M + \frac{3}{2a}\frac{d^2M}{d\varphi^2} + \frac{1}{2a}\frac{d^4M}{d\varphi^4}. \qquad (10)$$

Substitution of Eq. (10) in Eq. (9) yields the sixth order dynamic equation

$$-\frac{1}{2a}\frac{d^6M}{d\varphi^6}-\frac{1}{a}(1+\frac{a^2\omega^2}{2c_p^2})\frac{d^4M}{d\varphi^4}+(\frac{6a^3\omega^2}{h^2c_p^2}-\frac{1}{2a}+\frac{a\omega^2}{2c_p^2})\frac{d^2M}{d\varphi^2}-(1-\frac{a^2\omega^2}{c_p^2})\frac{6a^3\omega^2}{h^2c_p^2}M= \\ \frac{a}{2}(1+\frac{a^2\omega^2}{c_p^2})\frac{d^2p}{d\varphi^2}+\frac{a}{2}\frac{d^4p}{d\varphi^4}. \tag{11}$$

The latter equation indicates the existence of six homogeneous (i.e. $p\equiv 0$) waves $M=e^{-jk_s\varphi}$, whose wavenumbers k_s (s=1..6) are the solutions of the characteristic equation

$$\frac{1}{2a}k_s^6-\frac{1}{a}(1+\frac{a^2\omega^2}{2c_p^2})k_s^4-(\frac{6a^3\omega^2}{h^2c_p^2}-\frac{1}{2a}+\frac{a\omega^2}{2c_p^2})k_s^2-(1-\frac{a^2\omega^2}{c_p^2})\frac{6a^3\omega^2}{h^2c_p^2}=0. \tag{12}$$

Consequently, the general homogeneous solution may be expressed as

$$\begin{Bmatrix} v \\ w \\ \frac{dw}{d\varphi} \\ N \\ M \\ Q \end{Bmatrix} = \mathbf{H}.\begin{Bmatrix} A_1e^{-jk_1\varphi} \\ A_2e^{-jk_2\varphi} \\ A_3e^{-jk_3\varphi} \\ A_4e^{-jk_4\varphi} \\ A_5e^{-jk_5\varphi} \\ A_6e^{-jk_6\varphi} \end{Bmatrix} \tag{13}$$

with $$\mathbf{H}=\begin{bmatrix} v^{(1)} & v^{(2)} & v^{(3)} & v^{(4)} & v^{(5)} & v^{(6)} \\ w^{(1)} & w^{(2)} & w^{(3)} & w^{(4)} & w^{(5)} & w^{(6)} \\ -jk_1w^{(1)} & -jk_2w^{(2)} & -jk_3w^{(3)} & -jk_4w^{(4)} & -jk_5w^{(5)} & -jk_6w^{(6)} \\ N^{(1)} & N^{(2)} & N^{(3)} & N^{(4)} & N^{(5)} & N^{(6)} \\ \frac{1}{jk_1a} & \frac{1}{jk_2a} & \frac{1}{jk_3a} & \frac{1}{jk_4a} & \frac{1}{jk_5a} & \frac{1}{jk_6a} \end{bmatrix}, \tag{14}$$

where A_s (s=1,...,6) are arbitrary constants, $N^{(s)}=\dfrac{1}{1-\dfrac{a^2\omega^2}{c_p^2}}(-\dfrac{3k_s^2}{2a}+\dfrac{k_s^4}{2a}-\dfrac{6a^3\omega^2}{h^2c_p^2})$,

$$v^{(s)}=\frac{jk_s}{\rho ha\omega^2}(N^{(s)}+\frac{1}{a}) \text{ and } w^{(s)}=\frac{1}{\rho ha\omega^2}(N^{(s)}+\frac{k_s^2}{a}) \text{ , (s=1,..,6).} \tag{15}$$

2.2. Formulation of the coupled problem

Consider a finite acoustic domain with boundary surface Γ_a containing a cylindrical shell section Γ_s ($\Gamma_s \subseteq \Gamma_a$) (see Fig. 2). The shell section has a radius a, an arc length $a\Phi$ and its centre point is located at (x_0,y_0). A mechanical point force F is applied normal to the shell

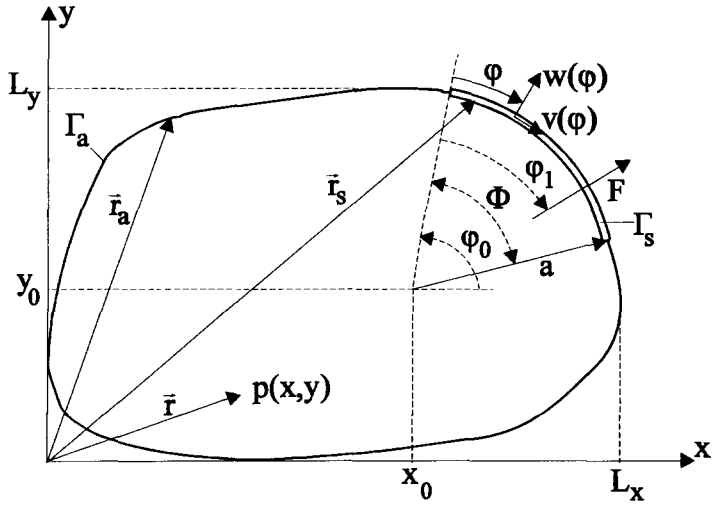

Fig. 2: vibro-acoustic system with cylindrical shell section

section at the angular position $\varphi = \varphi_1$. The steady-state acoustic pressure p at any point $\vec{r}(x,y)$ of an inviscid, homogeneous fluid is governed by the Helmholtz wave equation

$$\nabla^2 p(\vec{r}) + k^2 p(\vec{r}) = 0, \quad (16)$$

with k being the acoustic wavenumber ($k=\omega/c$), ω the circular frequency of the applied force and c the speed of sound in the fluid.

The steady-state bending moment M of the shell is governed by the dynamic equation (11), in which the excitation function p.a is extended with a force excitation term, ($\varphi \in [0,\Phi]$)

$$p(\vec{r}_s).a + F.\delta(\varphi-\varphi_1) = p(x_0 + a.\cos(\varphi_0-\varphi), y_0 + a.\sin(\varphi_0-\varphi)).a + F.\delta(\varphi-\varphi_1) \quad . \quad (17)$$

All other dynamic quantities (v, w, dw/dφ, N, Q) in the shell section result from the back-substitution of the obtained solution M(φ) in Eqs. (3-10).

Since the normal fluid displacement equals the radial shell displacement at the fluid-structure interface, the pressure field must satisfy the boundary condition

$$\nabla p(\vec{r}).\vec{n}_s(\vec{r}) = \rho_f \omega^2 w(\vec{r}), \quad \vec{r} \in \Gamma_s \, , \quad (18)$$

where ρ_f is the fluid density and $\vec{n}_s$ is the unit normal vector of the shell, directed outwards from the acoustic domain. In order to uniquely define the acoustic response, the boundary conditions at the remaining part of the acoustic boundary surface must be satisfied,

$$L_{a,b}[p(\vec{r})] = \tilde{g}_a(\vec{r}), \quad \vec{r} \in (\Gamma_a \setminus \Gamma_s) \, . \quad (19)$$

$L_{a,b}$ is a differential operator of maximum order 1 and $\tilde{g}_a$ is a prescribed function. Since the shell dynamic response is governed by a sixth order equation, three boundary conditions must be satisfied at each edge point of the shell ($\varphi = 0$ and $\varphi = \Phi$).

2.3. Wave representation

The basic idea of the wave based prediction technique is to express the steady-state response in terms of plane wave functions, extended with particular solutions, so that the governing equations are exactly satisfied.

For the case of a convex acoustic domain, the pressure field p, governed by the homogeneous wave equation (16), is expressed as a combination of generalised acoustic wave functions[3]

$$p(x,y)=\sum_a P_a\phi_a(x,y)=\sum_m P_m\cos(k_{xm}x)e^{-jk_{ym}(y-f_mL_y)}+\sum_n P_n e^{-jk_{xn}(x-f_nL_x)}\cos(k_{yn}y) \quad (20)$$

$$\text{with}\,(k_{xm},k_{ym})=(\frac{m\pi}{L_x},\pm\sqrt{k^2-k_{xm}^2})\,\text{and}\,(k_{xn},k_{yn})=(\pm\sqrt{k^2-k_{yn}^2},\frac{n\pi}{L_y}),\ (m,n=0,1,\ldots),$$

where L_x and L_y are the dimensions of the smallest rectangular domain which encloses the convex acoustic domain (see Fig. 2) and the constants f_m and f_n are defined as

$$f_m=\begin{cases}0, \text{ if } \mathrm{Im}(k_{ym})\le 0\\ 1, \text{ if } \mathrm{Im}(k_{ym})>0\end{cases},\quad f_n=\begin{cases}0, \text{ if } \mathrm{Im}(k_{xn})\le 0\\ 1, \text{ if } \mathrm{Im}(k_{xn})>0\end{cases}. \quad (21)$$

Since the shell dynamic equation has two inhomogeneous terms (one from the point force excitation and one from the acoustic pressure loading), the vector of dynamic quantities $\mathbf{x}_s=\left\{v,w,\frac{dw}{d\varphi},N,M,Q\right\}^T$ is expressed as a combination of homogeneous solutions, extended with two particular solutions,

$$\mathbf{x}_s(\varphi)=\mathbf{x}_{s,\mathrm{hom}}(\varphi)+\mathbf{x}_{s,\mathrm{part1}}(\varphi)+\mathbf{x}_{s,\mathrm{part2}}(\varphi),\quad \varphi\in[0,\Phi]. \quad (22)$$

According to Eq. (13), the homogeneous solution is proposed as

$$\mathbf{x}_{s,\mathrm{hom}}(\varphi)=\begin{Bmatrix}v(\varphi)\\ w(\varphi)\\ \frac{dw(\varphi)}{d\varphi}\\ N(\varphi)\\ M(\varphi)\\ Q(\varphi)\end{Bmatrix}_{\mathrm{hom}}=\mathbf{H}.\begin{Bmatrix}A_1e^{-jk_1(\varphi-f_1\Phi)}\\ A_2e^{-jk_2(\varphi-f_2\Phi)}\\ A_3e^{-jk_3(\varphi-f_3\Phi)}\\ A_4e^{-jk_4(\varphi-f_4\Phi)}\\ A_5e^{-jk_5(\varphi-f_5\Phi)}\\ A_6e^{-jk_6(\varphi-f_6\Phi)}\end{Bmatrix},\quad f_s=\begin{cases}0, \text{ if } \mathrm{Im}(k_s)\le 0\\ 1, \text{ if } \mathrm{Im}(k_s)>0\end{cases}\quad (s=1,..,6). \quad (23)$$

The particular solutions are based on the dynamic response $\tilde{\mathbf{x}}_s$ of a complete cylindrical shell due to a normal point force F applied at angular position φ=0,

$$\tilde{\mathbf{x}}_s(\varphi)=\begin{Bmatrix}\tilde{v}(\varphi)\\ \tilde{w}(\varphi)\\ \frac{d\tilde{w}(\varphi)}{d\varphi}\\ \tilde{N}(\varphi)\\ \tilde{M}(\varphi)\\ \tilde{Q}(\varphi)\end{Bmatrix}=\mathbf{H}.\begin{Bmatrix}\tilde{A}_1e^{-jk_1(\varphi-f_1 2\pi)}\\ \tilde{A}_2e^{-jk_2(\varphi-f_2 2\pi)}\\ \tilde{A}_3e^{-jk_3(\varphi-f_3 2\pi)}\\ \tilde{A}_4e^{-jk_4(\varphi-f_4 2\pi)}\\ \tilde{A}_5e^{-jk_5(\varphi-f_5 2\pi)}\\ \tilde{A}_6e^{-jk_6(\varphi-f_6 2\pi)}\end{Bmatrix},\quad \varphi\in[0,2\pi], \quad (24)$$

where the six constants $\tilde{A}_s$ (s=1,..,6) result from the six boundary conditions

$$\tilde{w}(0)=\tilde{w}(2\pi),\ \tilde{v}(0)=\tilde{v}(2\pi),\ \frac{d\tilde{w}(0)}{d\varphi}=\frac{d\tilde{w}(2\pi)}{d\varphi},$$
$$\tilde{N}(0)=\tilde{N}(2\pi),\ \tilde{M}(0)=\tilde{M}(2\pi)\ \text{ and }\ \tilde{Q}(0)-\tilde{Q}(2\pi)=F. \tag{25}$$

The response of a complete cylindrical shell (Eq. (24)) due to a point force excitation at $\varphi=\varphi_1$ is selected as particular solution for the point force excitation on the considered shell section,

$$\mathbf{x}_{s,part1}(\varphi)=\tilde{\mathbf{x}}_s(\mathrm{mod}(\varphi-\varphi_1,2\pi)),\ \ \varphi\in[0,\Phi], \tag{26}$$

where mod(*,2π) denotes the congruence modulo 2π. The response of a complete cylindrical shell due to a pressure loading along the section $\varphi\in[0,\Phi]$, which is identical to the pressure loading occurring in the considered vibro-acoustic system, is selected as particular solution,

$$\mathbf{x}_{s,part2}(\varphi)=\int_0^{\Phi} a.p(\vec{r}_\xi).\tilde{\mathbf{x}}_s(\mathrm{mod}(\varphi-\xi,2\pi)).d\xi\ ,\quad \varphi\in[0,\Phi], \tag{27}$$

$$\text{with}\ \ p(\vec{r}_\xi)=\sum_m P_m\cos(k_{xm}(x_0+a.\cos(\varphi_0-\xi))).e^{-jk_{ym}((y_0+a.\sin(\varphi_0-\xi))-f_mL_y)}$$
$$+\sum_n P_n e^{-jk_{xn}((x_0+a.\cos(\varphi_0-\xi))-f_nL_x)}.\cos(k_{yn}(y_0+a.\sin(\varphi_0-\xi)))\ . \tag{28}$$

2.4. Solution procedure

The proposed dynamic responses p(x,y) (Eq. (20)) and $\mathbf{x}_s(\varphi)$ (Eq. (22)) are exact solutions of the governing dynamic equations, no matter what the values of the unknown wave contributions A_s, P_m, P_n (s = 1,..,6 and m,n = 0,1,..) are. The contributions are only determined by the structural and acoustic boundary conditions. The six structural boundary conditions are defined at discrete points (three at both edge points of the shell section) and can be used as such. The acoustic boundary conditions (Eqs. (18) and (19)) are defined at a certain boundary domain. Therefore, they are transformed into a discrete set of approximating equations by expressing them in a weighted residual formulation[3]

$$\int_{\Gamma_s}\mathcal{W}_{a1}.(\nabla p.\vec{n}_s-\rho_f\omega^2 w).d\Gamma+\int_{\Gamma_a\setminus\Gamma_s}\mathcal{W}_{a2}.(L_{a,b}[p]-\tilde{g}_a).d\Gamma=0, \tag{29}$$

where expressions (20) and (22) are used as p and w and $\mathcal{W}_{a1}$ and $\mathcal{W}_{a2}$ are weighting functions. These weighting functions are defined as

$$\mathcal{W}_{a1}=\alpha_1(\nabla\phi_a.\vec{n}_s)^*,\ \mathcal{W}_{a2}=\alpha_2(L_{a,b}[\phi_a])^*, \tag{30}$$

where the constant factors α_1 and α_2 are such that the integral functions in Eq.(29) have the dimension of acoustic energy density per unit pressure (* denotes the complex conjugate). Each acoustic wave function $\phi_a(x,y)$ of the wave expansion in Eq. (20) is used to construct a set of weighting functions $\mathcal{W}_{a1}$ and $\mathcal{W}_{a2}$, which are then used in Eq. (29). Solving the resulting

equations, together with the structural boundary equations, for the unknown wave contributions A_s, P_m and P_n and substituting these contributions into Eqs. (20) and (22), yield the prediction of the steady-state coupled response.

3. Numerical examples

3.1. fluid-loaded cylindrical shell section

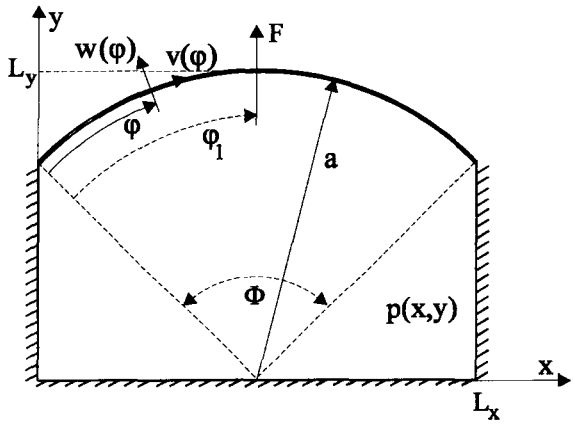

Fig. 3: fluid-loaded shell section

Consider the case of a point force excited cylindrical shell section, backed by an acoustic cavity, as shown on Fig. 3. The edges of the shell section are clamped to the rigid side walls of the cavity. The geometrical parameters are a = 0.707 m, $\Phi = \pi/2$ rad, h = 0.002 m, $\varphi_1 = \pi/4$ rad, L_x = 1m, L_y = a. The shell is made of aluminium (E = 70e+9 N/m^2, ν = 0.3 and ρ = 2790 kg/m^3) and the cavity is filled with air (c = 340 m/s, ρ_f = 1.225 kg/m^3). Due to the clamping of the shell, the six structural boundary conditions are

$$w(0) = v(0) = \frac{dw(0)}{d\varphi} = w(\Phi) = v(\Phi) = \frac{dw(\Phi)}{d\varphi} = 0. \qquad (31)$$

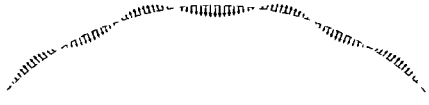

Fig. 4a : shell displacement at 230 Hz

Since three cavity side walls are rigid, the fluid displacement normal to these walls must be zero, so that $L_{a,b} = \nabla p.\vec{n}$ and $\tilde{g}_a = 0$ in the acoustic boundary condition (19).

Based on these boundary conditions, a wave model with 60 unknowns was constructed (6 structural and 54 (m=0,1,...,14;n=0,1,...,11) acoustic wave contributions). Figure 4a shows the resulting instantaneous shell displacement at 230 Hz. On figure 4b the radial shell displacement (solid line) at this frequency is plotted against the fluid displacement normal to the coupling interface (cross marks). Figure 4c shows the contour plot of the instantaneous cavity pressure. These figures clearly indicate that the small wave model is able to very accurately represent all structural and acoustic boundary conditions. Since the dynamic equations are always exactly satisfied, it may be concluded that the wave model enables a very accurate prediction of the dynamic response.

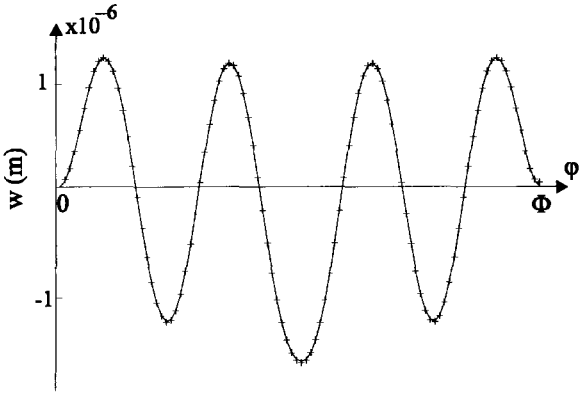

Fig. 4b: normal displacement continuity

In addition, two finite element models of this vibro-acoustic system were built. The first model consists of 20 linear shell and 200 linear fluid elements with a total of 288 unconstrained degrees of freedom. The

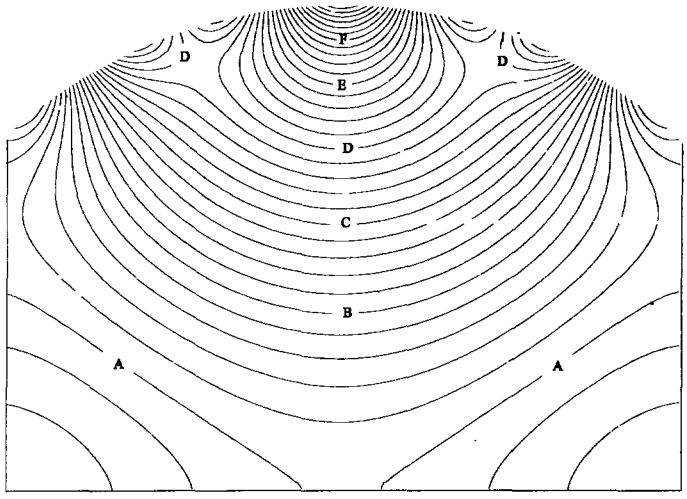

Fig. 4c : contour plot of instantaneous cavity pressure at 230 Hz

second model consists of 60 linear shell and 1800 linear fluid elements with a total of 2068 unconstrained degrees of freedom. The resulting radial displacement amplitudes at the excitation point and the acoustic pressure amplitudes at (x,y)=(0.5,0.4) due to a unit force F are shown on Figs. 5a and 5b, respectively. The thick solid lines represent the wave model results, while the results from the large finite element model are drawn in thin solid lines and those from the small finite element model in dotted lines. These figures clearly illustrate the effect of the mesh density on the accuracy. As mentioned in the introduction, the mesh density must be large enough to represent the spatial variation of the dynamic responses, which mostly depends on the wavelength. If not, the stiffness of the discretized system is overestimated, yielding too high resonance frequency predictions. Since the structural and acoustic wavelengths decrease for increasing frequency, this discretization error increases with frequency. As a result, a high mesh density is required to obtain a similar accuracy as the considerably smaller wave model. Note that the accuracy of the finite element predictions around 257 Hz, 348 Hz and 436 Hz is higher than around the other resonances. This is caused by the fact that most of the energy at these three resonances is stored in the acoustic cavity, while at the other resonances most of the energy is stored in the shell section. Since the acoustic wavelength is substantially larger than the structural wavelength, the discretization error is smaller for acoustically than for structurally dominated resonances.

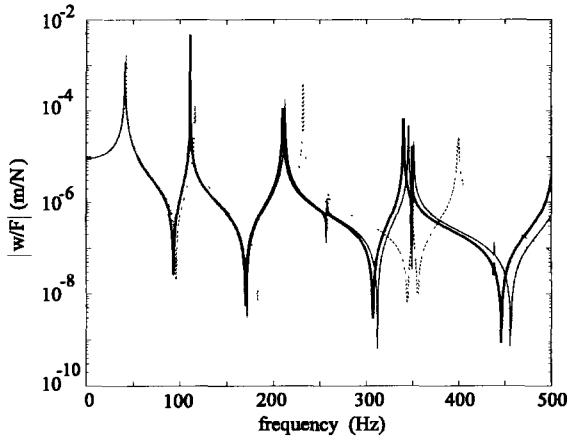

Fig. 5a : FRF of the radial displacement at the excitation point

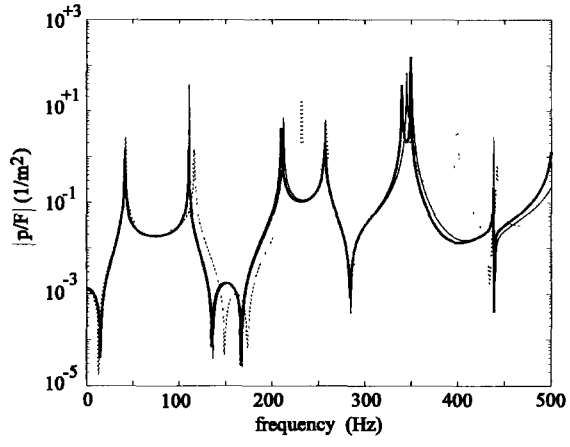

Fig. 5b : FRF of the cavity pressure at (x,y)=(0.5,0.4)m

3.2. *fluid-loaded cylinder*

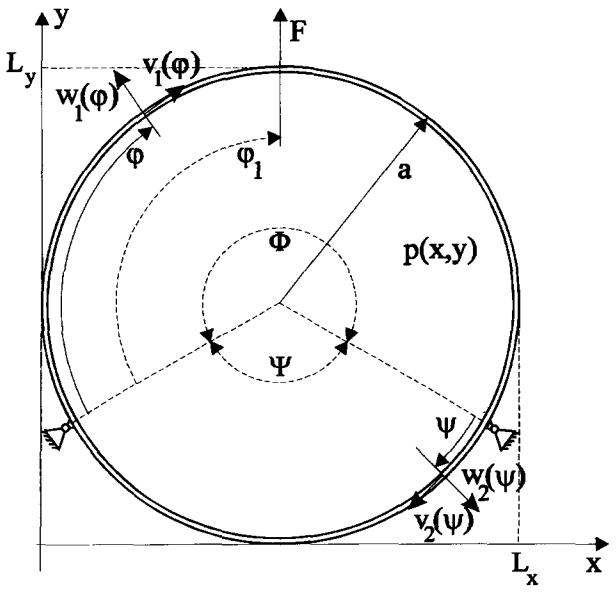

Fig. 6: fluid-loaded cylinder

Consider the case of a point force excited cylinder, which is supported at two points, as shown on Fig. 6. The cylinder is made of aluminium and the enclosed cavity is filled with air. The geometrical parameters are a = 0.25 m, $\Phi = 4\pi/3$ rad, h = 0.002 m, $\varphi_1 = 2\pi/3$ rad, $L_x = 2a$, $L_y = 2a$.

Since the wave based prediction method only can handle boundary conditions, the cylinder is split into two sections, one with arc length $a\Phi$ and one with arc length $a\Psi$. In this way, the effects of the supports on the dynamic response can be modelled as boundary conditions. Expression (22) is used for the dynamic quantities of the excited section; for the other section, the particular solution for the point force excitation is omitted in this expression. Since the cylinder is split in two sections, twelve instead of six structural boundary conditions must be satisfied,

$$w_1(0) = v_1(0) = w_1(\Phi) = v_1(\Phi) = w_2(0) = v_2(0) = w_2(\Psi) = v_2(\Psi) = 0,$$
$$\frac{dw_1(0)}{d\varphi} = \frac{dw_2(\Psi)}{d\psi}, \frac{dw_1(\Phi)}{d\varphi} = \frac{dw_2(0)}{d\psi}, M_1(0) = M_2(\Psi), M_1(\Phi) = M_2(0). \quad (32)$$

The acoustic boundary conditions are defined by the continuity of the radial shell displacement and the normal fluid displacement at the coupling interface with both sections.

A wave model with 60 unknowns was constructed (12 structural (6 per section) and 48 (m=0,1,...,11;n=0,1,...,11) acoustic wave contributions). The wave model results are compared with the results from two finite element models. The first model consists of 30 linear shell and 300 linear fluid elements with a total of 394 unconstrained degrees of freedom. The second model consists of 150 linear shell and 1500 linear fluid elements with a total of 1954 unconstrained degrees of freedom. The resulting radial displacement amplitudes at the excitation point and the acoustic pressure amplitudes at (x,y)=(0.25,0.4) due to a unit force F are shown on Figs. 7a and 7b, respectively. The same line types are used as in the previous numerical example. The same conclusions may be drawn. Due to the discretization error, a high mesh density is required to obtain a similar accuracy as the considerably smaller wave model. Again, the finite element results around the acoustically dominated resonances (399 Hz) are more accurate than the results around the structurally dominated ones.

4. Conclusions

In the finite element method, the dynamic variables are expressed in terms of simple, low order polynomial shape functions, which don't satisfy the governing dynamic equations nor boundary conditions. To obtain accurate results, the approximation error must be kept small by discretizing the considered continuous domain into a large number of elements, which

results in a large model size and subsequent computational effort. For coupled vibro-acoustic problems, the model size becomes even larger as the structural and acoustic problem must be solved simultaneously. Moreover, in a coupled finite element formulation, a non-symmetrical set of equations must be solved, which requires a substantially larger computational effort, compared to a symmetrical uncoupled structural or acoustic model.

This paper discusses the use of a wave based prediction technique for the steady-state coupled response of two-dimensional vibro-acoustic systems with cylindrical shell components. The structural and acoustic dynamic variables are expressed as a combination of plane structural and acoustic waves, which are exact solutions of the homogeneous wave equations. Structural and acoustic particular solutions are added to satisfy the inhomogeneous excitation terms. The contributions of the waves to the dynamic response are determined by applying the boundary conditions in a weighted residual formulation. In this way, the accuracy depends only on the approximation error, induced by the boundary conditions. In comparison with the finite element method, very accurate prediction results are obtained from a substantially smaller wave model, as illustrated for two numerical examples.

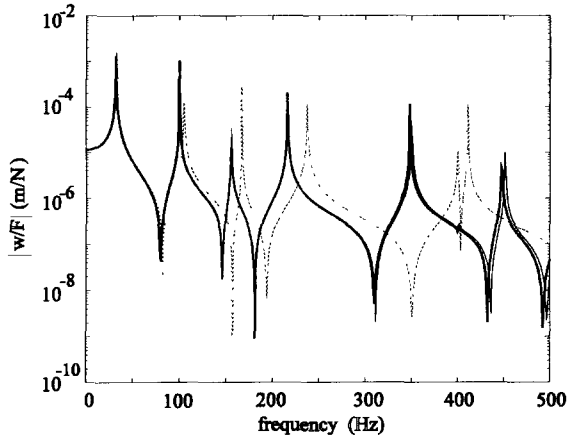

Fig. 7a: FRF of the radial displacement at the excitation point

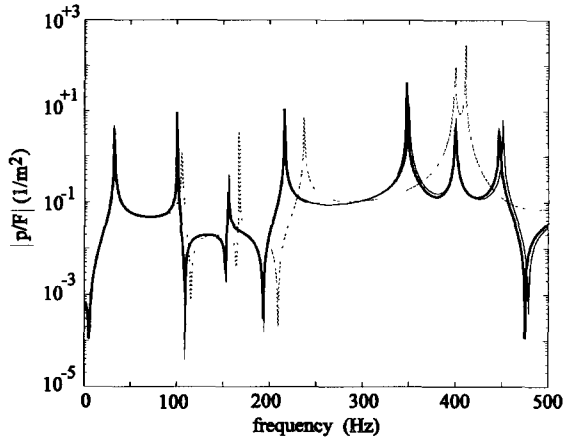

Fig. 7b: FRF of the cavity pressure at (x,y)=(0.25,0.4)m

References

1. O.C. Zienkiewicz and R.E. Newton, 'Coupled vibration of structures submerged in a compressible fluid', Proc. Int. Symp. Finite Element Techniques, University of Stuttgart, Germany, (1969).
2. W. Desmet, P. Sas and D. Vandepitte, 'A new wave based prediction technique for coupled vibro-acoustic analysis: theoretical description and application to a double wall structure', Proc. of ISMA 21, K.U.Leuven, Belgium, 105-134 (1996).
3. W. Desmet, P. Sas and D. Vandepitte, 'A wave based prediction technique for two-dimensional coupled vibro-acoustic analysis', submitted for publication in International Journal for Numerical Methods in Engineering.
4. W. Desmet, P. Sas and D. Vandepitte, 'How accurate does an impedance model represent porous acoustic insulation? A validation study using a new wave based prediction technique', Proc. Inter-noise 97, Technical University of Budapest, Hungary (1997).
5. A.E.H. Love, 'A treatise on the mathematical theory of elasticity', 4th ed., Dover Publications, New York (1944).